Directionally anisotropic Si nanowires: on-chip nonlinear grating devices in uniform waveguides

Jeffrey B. Driscoll,[1,*] Richard R. Grote,[1] Xiaoping Liu,[1] Jerry I. Dadap,[1]
Nicolae C. Panoiu,[2] and Richard M. Osgood, Jr.[1]

[1]*Microelectronics Sciences Laboratories, Columbia University, New York, New York 10027, USA*

[2]*Department of Electronic and Electrical Engineering, University College London, Torrington Place, London WC1E 7JE, UK*

**Corresponding author: jbd2112@columbia.edu*

Received January 7, 2011; revised March 4, 2011; accepted March 5, 2011;
posted March 8, 2011 (Doc. ID 140768); published April 13, 2011

Computational studies are used to show that the crystalline structure of Si causes the waveguide Kerr effective nonlinearity, γ, to vary by 10% for in-plane variation of the orientation of a silicon nanowire waveguide (SiNWG) fabricated on a standard silicon-on-insulator wafer. Our analysis shows that this angular dependence of γ can be employed to form a nonlinear Kerr grating in dimensionally uniform SiNWGs based on either ring resonators or cascaded waveguide bends. The magnitude of the nonlinear index variation in these gratings is found to be sufficient for phase matching in four-wave mixing and other optical parametric processes.

OCIS codes: 190.3270, 130.4310.

There has been recent, rapid growth in understanding and applying nonlinear optical phenomena in silicon (Si) nanowire waveguides (SiNWGs) fabricated on the Si-on-insulator (SOI) platform. The high index-of-refraction (n) contrast between the Si waveguiding region and surrounding cladding allows tightly confined guiding modes to be realized in devices with submicrometer transverse size [1,2]. This tight optical confinement, along with the high intrinsic third-order susceptibility of Si, results in an effective nonlinear coefficient, γ, which is $\sim 10^5$ times as large as that of optical fibers [3,4]. Many all-optical nonlinear devices based on this ultrafast nonlinearity have emerged [3,5], and thus it is increasingly important to understand the effect of material parameters on γ.

In this Letter we report the implications of waveguide orientation with respect to the Si crystallographic axes on the nonlinear properties of nanowires. Devices that take advantage of the anisotropic Si nonlinearity have recently been proposed, including an optical isolator [6] and a device designed for cavity-enhanced quasi-phase-matching [7,8], based on either the Kerr or Raman effect. Here we demonstrate that γ can vary by as much as 10% with waveguide orientation, allowing one to achieve periodic variations in γ by means of ringlike structures or cascaded waveguide bends (CWBs). These devices enable the formation of a nonlinear Kerr grating in guiding structures with uniform transverse section. We further propose phase matching a parametric process as a potential application for the formation of such a grating.

Si possesses an intrinsic anisotropic Kerr nonlinearity due to its crystalline structure [9,10], and as a result, the nonlinear optical properties of bulk Si are described rigorously by a third-order (electronic) susceptibility tensor, $\chi^{(3)}$, instead of a single scalar parameter. The tensor elements of $\chi^{(3)}$ are determined by first employing symmetry considerations to reduce $\chi^{(3)}$ to two independent elements ($\chi^{(3)}_{1111}$ and $\chi^{(3)}_{1122}$) [3,11], the ratio of which has been experimentally measured [9]. Therefore, $\chi^{(3)}$ can be completely characterized using knowledge of one element (for details see [3]). In order to determine γ, we obtain the effective nonlinear susceptibility, Γ, via

$$\Gamma = \frac{A_0 \int_{A_0} \boldsymbol{e}^*(\omega) \cdot \boldsymbol{\chi}^{(3)}(\boldsymbol{r}_\perp; -\omega, \omega, -\omega, \omega) \vdots \boldsymbol{e}(\omega)\boldsymbol{e}^*(\omega)\boldsymbol{e}(\omega)\mathrm{d}A}{\left(\int_{A_\infty} n^2(\boldsymbol{r}_\perp; \omega)|\boldsymbol{e}(\boldsymbol{r}_\perp; \omega)|^2 \mathrm{d}A\right)^2}, \quad (1)$$

where $A_0 = (h \times w)$ is the transverse section of the SiNWG, A_∞ is an infinite cross section, $\boldsymbol{r}_\perp$ represents transverse position, and $\boldsymbol{e}(\boldsymbol{r}_\perp; \omega)$ is the electric field of the waveguide mode. From Γ, γ is determined by

$$\gamma = (3\omega\Gamma')/(4\epsilon_0 A_0 v_g^2), \quad (2)$$

where Γ' is the real part of Γ, and v_g the group velocity [3,11]. All components of the electric field are included in this formulation, including the longitudinal field [12] and the anisotropy in optical nonlinearity through $\chi^{(3)}$. Slow-light enhancement via v_g is also explicitly accounted for, an important phenomenon in strongly dispersive photonic guiding structures [13].

One important property of γ revealed by Eqs. (1) and (2) is its dependence on waveguide orientation with respect to the principal axes of the Si crystal, whereas the linear guided modes depend only on the isotropic n. Consider the case of SiNWGs fabricated on a (001) wafer, the standard orientation of SOI device layers. For this example, we choose a typical $220\,\mathrm{nm} \times 500\,\mathrm{nm}$ (height $\times$ width) SiNWG with air top-cladding and calculate γ for different waveguide orientations. The waveguide is initially oriented with its x and z axes along the [110] and [$1\bar{1}0$] crystal direction, respectively [see Fig. 1(a)]; the waveguide is then rotated by π radians about the [001] direction. There are differing experimental reports pertaining to the degree of nonlinear anisotropy

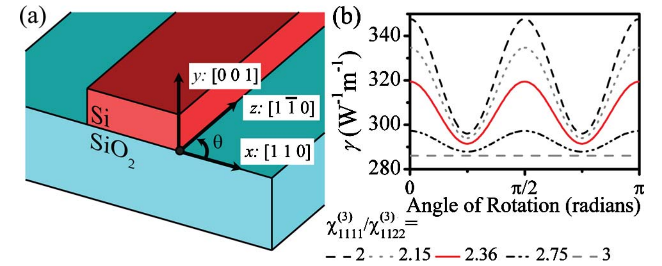

Fig. 1. (Color online) (a) Initial orientation of SiNWG with respect to Si crystal, (b) γ versus Si crystal rotation (about the [001] direction) for a $220\,\mathrm{nm} \times 500\,\mathrm{nm}$ SiNWG at $\lambda = 1.55\,\mu\mathrm{m}$. $\chi^{(3)}_{1111}/\chi^{(3)}_{1122} = 2$, 2.15, 2.36, 2.75, and 3 are considered.

exhibited by Si [9,14,15]; therefore, we consider ratios of $\chi^{(3)}_{1111}/\chi^{(3)}_{1122}$ between 2 and 3 for comparison (a ratio equal to 3 indicates no anisotropy). The results of this calculation show a cyclical change in γ with respect to the angle of rotation for all $\chi^{(3)}_{1111}/\chi^{(3)}_{1122}$ except $\chi^{(3)}_{1111}/\chi^{(3)}_{1122} = 3$ [Fig. 1(b)]. For the remainder of this Letter, we assume $\chi^{(3)}_{1111}/\chi^{(3)}_{1122} = 2.36$ as measured in [9]. For this anisotropy, the maximum (minimum) nonlinearity occurs for $\theta = m\pi/2$ ($\theta = (2m+1)\pi/4$), where m is an integer. The difference in γ between maximum ($\gamma_{\mathrm{MAX}} \sim 320\,\mathrm{W}^{-1}\,\mathrm{m}^{-1}$) and minimum ($\gamma_{\mathrm{MIN}} \sim 290\,\mathrm{W}^{-1}\,\mathrm{m}^{-1}$) is $\sim$10%.

A rotation about the [001] direction is of practical importance, since this rotation is equivalent to changing the orientation of the waveguide on the chip surface. For example, a continuous $\theta = \pi$ rotation is equivalent to a 180° bend on-chip, leading to a two-sinusoidal-cycle variation in γ [Fig. 1(b)]. This result also indicates that light propagating through a fully circular path, i.e., a ring resonator [Fig. 2(a)], experiences a sinusoidal variation in γ, which generates a nonlinear index grating in the presence of a pump, with a period, Λ_{NL}, given by

$$\Lambda_{\mathrm{NL}} = \pi R/2, \tag{3}$$

with R being the radius of the ring. This nonlinear optical grating can also be obtained through cascaded bends [see Fig. 2(b)], in which case Eq. (3) would still hold, provided that the bends are circular. The grating length in the case of CWBs ($L_{G,\mathrm{cwb}}$) is simply determined by the number of bends, N_B, via $L_{G,\mathrm{cwb}} = \pi R N_B$, limited by propagation loss. Note that our analysis ignores the influence of the waveguide bending on the field profile of the optical modes and, implicitly, on γ. Our calculations, however, show that for bends with $R > 5\,\mu\mathrm{m}$ this effect changes γ by <1%.

For the case of a ring resonator, the equivalent grating length is dependent on resonator quality factor, Q, via the photon lifetime. In this case, the number of round trips in the ring gives the equivalent unfolded optical grating length. More specifically, $L_{G,\mathrm{ring}} = N_R L_C = Q\lambda_0/(2\pi N_{\mathrm{G}})$, where $N_R = Q\lambda_0/(2\pi N_{\mathrm{G}} L_C)$ is the number of round trips for a mode in the ring prior to a $1/e$ intensity decrease [16], L_C is the ring circumference, N_{G} is the group index of the mode traveling in the ring, and λ_0 is the free-space wavelength. As an example, a ring with $R = 30\,\mu\mathrm{m}$, $Q = 45{,}000$, and $N_{\mathrm{G}} = 3.48$ at $\lambda_0 = 1.512\,\mu\mathrm{m}$ [17] would give $L_G = 3.11\,\mathrm{mm}$ and $\Lambda_{\mathrm{NL}} = 47.12\,\mu\mathrm{m}$, producing a long-period grating with 66 periods spaced by Λ_{NL}. To produce a shorter period grating, a smaller ring R would be required. In fact, very small rings ($R < 1.5\,\mu\mathrm{m}$) with high Q values have been realized on the SOI platform [18], where these rings would form gratings with $\Lambda_{\mathrm{NL}} \sim 2\,\mu\mathrm{m}$.

The grating strength is directly related to the waveguide peak power, P_p. The grating index differential (Δn) can be estimated by $\Delta n = cP_p(\gamma_{\mathrm{MAX}} - \gamma_{\mathrm{MIN}})/\omega$. As an example, Fig. 2(c) shows the resulting Δn as a function of pump P_p. Typical peak pulsed-pump powers in SiNWG experiments vary from 1 to 1000 W; these result in values of Δn between 10^{-5} and 10^{-2}. Gratings with this Δn can be useful for on-chip signal processing applications such as switching, routing, mode coupling, or phase matching [19,20]. Note that for the case of high P_p, a more detailed analysis that included nonlinear absorption and dispersion would be required to determine the precise Δn along the unfolded grating.

As an example of a specific application of such a nonlinear grating, consider (degenerate) four-wave mixing (FWM) in a $220\,\mathrm{nm} \times 500\,\mathrm{nm}$, $L = 0.5\,\mathrm{cm}$ SiNWG. Finite element calculations show that such a waveguide is highly dispersive near $\lambda = 1.55\,\mu\mathrm{m}$ with a large group-velocity dispersion coefficient of $\beta_2 \approx -3.3\,\mathrm{ps}^2\,\mathrm{m}^{-1}$, which limits the FWM conversion bandwidth ($\Delta\lambda$). In fact, for this value of β_2, $\Delta\lambda \approx [\lambda^4/(\pi c^2 \beta_2 L)]^{1/2} \approx 35\,\mathrm{nm}$ in the small-gain regime [21]. Consider also a pump ($\lambda_p = 1.55\,\mu\mathrm{m}$) and signal ($\lambda_s = 1.8\,\mu\mathrm{m}$), chosen to be separated spectrally (250 nm) by $\gg$ the conversion bandwidth. Energy conservation shows that the resulting idler is at $\lambda_i = (2\lambda_p^{-1} - \lambda_s^{-1})^{-1} = 1.361\,\mu\mathrm{m}$. In the absence of any grating the nonlinear interaction is not phase matched, with the corresponding phase mismatch, $\Delta\beta$, being expressed by $\Delta\beta = 2\gamma P_p - (2\beta_p - \beta_s - \beta_i)$, where $\beta_{p,s,i}$ is the propagation constant of the pump, signal, and

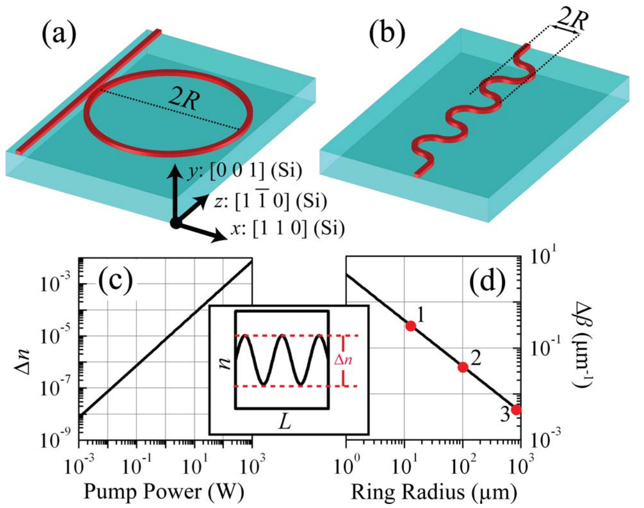

Fig. 2. (Color online) Nonlinear optical grating on-chip via (a) ring resonator or (b) CWBs. (c) Δn (as defined in inset) experienced by the pump formed by nonlinear grating versus P_p. A copropagating signal would experience $2\Delta n$ due to cross-phase modulation [4]. (d) $\Delta\beta$ compensated by a grating formed in a ring resonator or CWBs of varying R. Points 1, 2, and 3 give examples of phase matching with a 100 mW pump at $\lambda_p = 1.55\,\mu\mathrm{m}$ and R, λ_s, and λ_i of (1) 20.7, 2, and $1.265\,\mu\mathrm{m}$; (2) 100, 1.714, and $1.415\,\mu\mathrm{m}$; and (3) 900, 1.601, and $1.502\,\mu\mathrm{m}$, respectively.

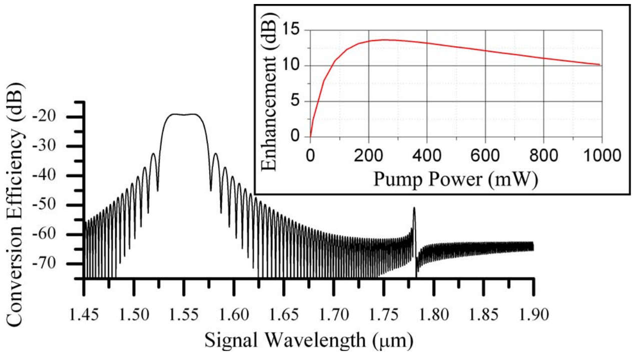

Fig. 3. (Color online) Conversion efficiency for varying λ_s in CWBs with $R = 47.98\,\mu$m and $\lambda_p = 1.55\,\mu$m. A ~12 dB enhancement occurs for $\lambda_s = 1.78\,\mu$m. The inset plots the conversion efficiency enhancement as a function of pump power.

idler, respectively. Assuming $P_p = 100\,$mW [21], $\Delta\beta = 0.0834\,\mu\text{m}^{-1}$. However, a nonlinear grating can compensate this phase mismatch if $\Lambda_{\text{NL}} = 2\pi/|\Delta\beta|$, which is satisfied if $\Lambda_{\text{NL}} = 75.37\,\mu$m, and realizable by a ring resonator or CWBs with $R = 47.98\,\mu$m.

The conversion efficiency improvement resulting from this particular grating can be illustrated by performing a rigorous FWM calculation that takes into account Kerr effects, two-photon absorption (TPA), free carrier absorption (FCA), free carrier dispersion, and linear loss. Considering the same SiNWG, exhibiting 1 dB/cm propagation loss and a 0.5 ns free carrier lifetime, we calculate the conversion efficiency (defined as the ratio between the output idler power and input probe power) for a pump ($\lambda_p = 1.55\,\mu$m), signal, and idler with coupled powers of 100, 1, and 0 mW respectively for varying λ_s. The nonlinear grating is taken into account through the anisotropy of Γ and assuming CWBs with $R = 47.98\,\mu$m. The result is shown in Fig. 3, where a sharp conversion efficiency enhancement of ~12 dB is shown near the target probe wavelength. The inset of Fig. 3 quantifies how the conversion efficiency enhancement varies with pump power, demonstrating that the 100 mW pump power used here is near the limit for the maximum enhancement achievable for the CW case at these wavelengths due to optical limiting, which saturates the optical power as a result of TPA and FCA [3]. This saturation can be ameliorated by moving $\lambda_p > 2.2\,\mu$m to avoid TPA altogether [22], leading to higher conversion efficiency.

An equivalent method has recently been proposed for phase matching FWM in a ring using the anisotropic Kerr effect [7]; however, the use of a ring, as compared to CWBs, can pose a practical challenge, since all signals would additionally have to meet the ring resonance condition. Figure 2(d) shows that a nonlinear grating formed with a ring resonator or CWBs of varying R can compensate a wide range of $\Delta\beta$, illustrating the broad wavelength range that can be phase matched using this method. Further, this approach is not restricted to periodic variations of γ but can be employed to achieve virtually any predesigned spatial dependence $\gamma = \gamma(z)$, such as an apodized grating, limited by bending loss.

We acknowledge support from a National Science Foundation (NSF)/Engineering and Physical Sciences Research Council (EPSRC) Materials World Network Grant.

References

1. R. U. Ahmad, F. Pizzuto, G. S. Camarda, R. L. Espinola, H. Rao, and R. M. Osgood, Jr., IEEE Photon. Technol. Lett. **14**, 65 (2002).
2. Y. A. Vlasov and S. J. McNab, Opt. Express **12**, 1622 (2004).
3. R. M. Osgood, Jr., N. C. Panoiu, J. I. Dadap, X. Liu, X. Chen, I. W. Hsieh, E. Dulkeith, W. M. Green, and Y. A. Vlasov, Adv. Opt. Photon. **1**, 162 (2009).
4. G. P. Agrawal, *Nonlinear Fiber Optics*, 4th ed. (Elsevier, 2007).
5. Q. Lin, O. J. Painter, and G. P. Agrawal, Opt. Express **15**, 16604 (2007).
6. M. Krause, H. Renner, and E. Brinkmeyer, Electron. Lett. **44**, 691 (2008).
7. N. Vermeulen, J. E. Sipe, C. Debaes, and H. Thienpont, in *2010 IEEE Photonics Society Summer Topical Meeting Series* (IEEE, 2010), pp. 92–93.
8. N. Vermeulen, J. E. Sipe, and H. Thienpont, IEEE Photon. Technol. Lett. **22**, 1796 (2010).
9. J. Zhang, Q. Lin, G. Piredda, R. W. Boyd, G. P. Agrawal, and P. M. Fauchet, Appl. Phys. Lett. **91**, 071113 (2007).
10. M. P. Chethiya, M. Dissanayake, I. D. Rukhlenko, and G. P. Agrawal, Opt. Express **18**, 21427 (2010).
11. X. G. Chen, N. C. Panoiu, and R. M. Osgood, Jr., IEEE J. Quantum Electron. **42**, 160 (2006).
12. J. B. Driscoll, X. P. Liu, S. Yasseri, I. Hsieh, J. I. Dadap, and R. M. Osgood, Jr., Opt. Express **17**, 2797 (2009).
13. N. C. Panoiu, J. F. McMillan, and C. W. Wong, IEEE J. Sel. Top. Quantum Electron. **16**, 257 (2010).
14. M. Dinu, F. Quochi, and H. Garcia, Appl. Phys. Lett. **82**, 2954 (2003).
15. J. O'Dowd, W. H. Guo, M. Lynch, E. Flood, A. L. Bradley, and J. F. Donegan, Electron. Lett. **46**, 854 (2010).
16. D. G. Rabus, *Integrated Ring Resonators*, Vol. 127 of Springer Series in Optical Sciences (Springer, 2007).
17. T. Baehr-Jones, M. Hochberg, C. Walker, and A. Scherer, Appl. Phys. Lett. **85**, 3346 (2004).
18. Q. F. Xu, D. Fattal, and R. G. Beausoleil, Opt. Express **16**, 4309 (2008).
19. A. M. Vengsarkar, P. J. Lemaire, J. B. Judkins, V. Bhatia, T. Erdogan, and J. E. Sipe, J. Lightwave Technol. **14**, 58 (1996).
20. J. Kim, O. Boyraz, J. H. Lim, and M. N. Islam, J. Lightwave Technol. **19**, 247 (2001).
21. M. A. Foster, A. C. Turner, R. Salem, M. Lipson, and A. L. Gaeta, Opt. Express **15**, 12949 (2007).
22. X. Liu, R. M. Osgood, Jr., Y. A. Vlasov, and W. M. J. Green, Nat. Photon. **4**, 557 (2010).